



Proceeding Paper

Functionalization and Characterization of New Chitosan Derivatives Obtained by 1,3-Dipolar Cycloaddition Reaction (CuAAC) [†]

Johana Gutierrez-Guzmán *, Christian David Alcívar-León *, Verónica Jeanneth Taco-Taco, Ronny Flores and Pablo M. Bonilla-Valladares

Facultad de Ciencias Químicas, Universidad Central del Ecuador, Francisco Viteri s/n y Gilberto Gato Sobral, Quito 170521, Ecuador; vjtaco@uce.edu.ec (V.J.T.-T.); raflores@uce.edu.ec (R.F.); pmbonilla@uce.edu.ec (P.M.B.-V.)

- * Correspondence: mjgutierrez@uce.edu.ec (J.G.-G.); cdalcivar@uce.edu.ec (C.D.A.-L.)
- † Presented at the 29th International Electronic Conference on Synthetic Organic Chemistry (ECSOC-29); Available online: https://sciforum.net/event/ecsoc-29.

Abstract

Chitosan is a biopolymer with excellent properties such as biodegradability, biocompatibility, bioactivity, and non-toxicity, making it an attractive material for various applications. In this study, to enhance these properties particularly for the development of food coatings chitosan derivatives (1,2,3-triazoles) were synthesized via microwave-assisted 1,3-dipolar cycloaddition (CuAAC) using different terminal alkynes. The resulting compounds were obtained in high yields 79.7–88.0% and characterized by vibrational (IR) and electronic (UV–Visible) spectroscopy. Films were formed by combining the derivatives with PVA and characterized using differential scanning calorimetry (DSC), tensile strength testing, and water vapor permeability analysis. The resulting films exhibited improved mechanical properties, homogeneous thicknesses, low-porosity surfaces, and favorable barrier properties, highlighting their potential applicability as food coating materials.

Keywords: chitosan; 1,3-dipolar cycloaddition; food coatings

Academic Editor(s): Name

Published: date

Citation: Gutierrez-Guzmán, J.; Alcívar-León, C.D.; Taco-Taco, V.J.; Flores, R.; Bonilla-Valladares, P.M. Functionalization and Characterization of New Chitosan Derivatives Obtained by 1,3-Dipolar Cycloaddition Reaction (CuAAC). Chem. Proc. 2025, volume number, x. https://doi.org/10.3390/xxxxx

Copyright: © 2025 by the authors. Submitted for possible open access publication under the terms and conditions of the Creative Commons Attribution (CC BY) license (https://creativecommons.org/license s/by/4.0/).

1. Introduction

Chitosan is a natural polymer valued for its aqueous acid solubility, biodegradability, biocompatibility, bioactivity, and non-toxicity [1,2]. Its derivatives exhibit tunable thermoresponsive, photochromic, and pH-sensitive properties, often modified at primary amino groups, which may affect antimicrobial bioadhesion [3]. Click chemistry, particularly copper-catalyzed 1,3-dipolar cycloaddition (Cu-AAC) between alkynes and azides [4,5], efficiently generates 1,2,3-triazoles under mild conditions (Scheme 1), providing a versatile route for new chitosan derivatives.

Chem. Proc. 2025, x, x https://doi.org/10.3390/xxxxx

Scheme 1. Catalytic cycle of the 1,3-dipolar cycloaddition reaction catalyzed by copper CuAAC.

2. Materials and Methods

2.1. Materials and Reagents

Chitosan (CS) from shrimp shells (DD 90.9%, solubility 84.1%) was obtained as previously reported [6], acetic acid (ACS, ≥99.7%), hydrochloric acid (ACS, 37%), diethyl ether, hexadecyltrimethylammonium bromide (CTAB), sodium azide, epichlorohydrin, poly(vinyl alcohol) (PVA). All solvents and reagents were purchased from Sigma-Aldrich and used without further purification.

2.2. General

The FTIR spectra were recorded using a JASCO FT/IR-4600 equipped with attenuated total reflectance (ATR), with a resolution of 2.0 cm⁻¹, over a spectral range of 4000 cm⁻¹ to 400 cm⁻¹. UV-Vis spectra were using a Varian Cary 50 Bio UV-Vis Spectrophotometer with a spectral range of 190 nm to 800 nm. Theoretical studies were conducted using the Gaussian 09 software package, and the results were visualized with the Gauss View 6.0 interface.

2.3. Synthesis of 4-Azido-1-chlorobutan-2-ol (1)

CTAB (1.6 mmol) was dissolved in distilled water (40 mL) in an amber vessel, followed by sodium azide (2.5×10^2 mmol). After complete dissolution, epichlorohydrin (2.6×10^2 mmol) was added and stirred for 24 h at room temperature. The product (1) (18.9 g) was washed with diethyl ether, separated by funnel, and dried at room temperature.

2.4. Synthesis of Azido-Modified Chitosan (2)

Chitosan (9.09 mmol) was dissolved in 100 mL of 5% HCl–acetic acid (1:10 v/v), followed by the addition of compound 1 (7.3 × 10¹ mmol) and sonication for 4 h under light protection. The product (2) with an 89.6% yield (1.3 g) was precipitated with 40% ammonium hydroxide in methanol, filtered, washed (methanol, water, diethyl ether), vacuum-dried (24 h), and stored in the dark.

2.5. Synthesis of Functionalized Chitosan Derivatives (1,2,3-Triazoles)

Compound 2 (1.34×10^{-3} mmol) was reacted with various terminal alkynes under CuAAC conditions (Table 1). Reactions were carried out with CuSO₄ (1.1×10^{-2} mmol)/ascorbic acid (2.1×10^{-2} mmol) catalyst in aqueous medium (CH3COOH 1%, 20 mL) at room temperature (Scheme 2). The products were collected by filtration, washed, and dried. Compounds 3, a–f were obtained as solid

Scheme 2. Synthesis of functionalized chitosan derivatives by azide-alkyne cycloaddition reaction.

Table 1. Alkynes used in synthesis of functionalized chitosan derivatives.

Alkynes	Compound (3)	Alkyne Used (mmol)	Yield (%)
p-ethynyl toluene	CS-TOL (a)	4.3×10^{-1}	88.0
1-bromo-4-ethynylbenzene	CS-Br (b)	2.8×10^{-1}	82.6
2-ethynyl-1,3,5-trimethylbenzene	CS-CH ₃ (c)	3.5×10^{-1}	82.0
4-ethynylbenzaldehyde	CS-CHO (d)	3.8×10^{-1}	83.0
4-ethynyl- α , α , α -trifluorotoluene	CS-CF ₃ (e)	2.9×10^{-1}	79.7
acetonitrile	CS-ACN (f)	1.2	85.3

2.6. Theoretical Study

Geometry optimizations and theoretical IR spectra calculations were performed using Gaussian 09 software for compounds **1** and **2**, as well as for the monomers of chitosan and compounds **3a–f**. The density functional theory (DFT) method with the B3LYP/6-31G level of theory was applied.

2.7. Films Preparation

Films were prepared by solvent casting. Compounds 3a-f (1% acetic acid) and PVA (5%) solutions were sonicated (10 min, 25 °C), mixed 1:1, and stirred for 15 min. The blends were cast into Petri dishes, dried at 36 °C for 24 h, peeled off, and stored in desiccators.

2.8. Characterization of Films

2.8.1. Thermal Stability

Differential scanning calorimetry (DSC) was performed using a TA Instruments Q200, following the procedure reported by Ullah [7] with modifications. A 2 mg film sample was cut and placed into an aluminum pan. The analysis was performed with a continuous purge of nitrogen gas at a flow rate of 40 mL/min with a heating rate of 10 °C/min⁻¹ in the temperature range of 50 to 450 °C. The characteristic transition temperatures values were recorded.

2.8.2. Physical Properties (Thickness)

The thickness of each film type was measured using a HELIOS-PREISSER micrometer. Measurements were taken at five different points of each film.

2.8.3. Mechanical Properties

Films (100×10 mm) were tested for tensile strength using a universal testing machine (Shimidzu, AGSX) with an initial grip separation of 5 mm and a crosshead speed of 5 mm/min. Tests were performed in triplicate at room temperature.

2.8.4. Topographic Analysis

The roughness and surface topography of the films were analyzed using an atomic force microscope (Park Systems, model NX10). The instrument was operated in contact mode with a set point of 180 nm between the silicon nitride cantilever tip and the sample. Portions measuring $1 \text{ cm} \times 1 \text{ cm}$ were cut from each film, and their surfaces were mapped.

2.8.5. Water Vapor Permeability (WVP)

The methodology described by Cazón [8] was used with modifications. A 15 mL Falcon tube was filled with 3 mL of water, covered with the film, weighed, and placed in a desiccator. Weight loss was recorded every 30 min for 7 h. WVP was calculated using Equation (1):

$$WVP = \frac{\Delta w \times T}{\Delta t \times A \times \Delta P} \tag{1}$$

where $\Delta w/\Delta t$ is the weight loss rate (g/s), T the film thickness (m), A the exposed area (m²), and ΔP the vapor pressure differential (1017 Pa at 15 °C).

3. Results and Discussion

3.1. Synthesis

3.1.1. Synthesis of Azidated Chitosan

The synthesis of compound **2** was a sucessefull with a good yield of 89.55. IR spectrum of azidated chitosan (Figure 1b) exhibited a strong band at 2106 cm⁻¹, which was absent in the IR spectrum of native chitosan (Figure 1a). This band is characteristic of the azide group, confirming the successful functionalization of chitosan.

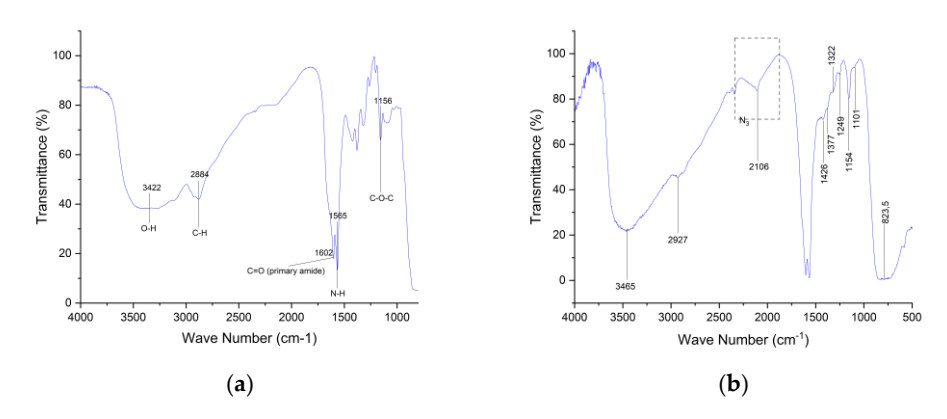


Figure 1. IR spectrum: (a) Chitosan; (b) Azidated chitosan.

3.1.2. Synthesis of Functionalized Chitosan Derivatives (1,2,3-Triazoles)

Compounds **3a–f** were obtained in high yields (Table 1). This is consistent with the copper-catalyzed azide–alkyne cycloaddition (CuAAC) reaction, which typically proceeds with high yields and excellent regioselectivity, converting organic azides and terminal alkynes into 1,4-disubstituted 1,2,3-triazoles. The reaction follows a catalytic mechanism involving multiple copper–organic intermediates (Scheme 1).

3.2. Derivatives Characterization

UV-Visible and IR Spectroscopy

The theoretical and experimental IR spectra of the derivatives showed the disappearance of the azide (N₃) peak at 2106 cm⁻¹ (Figure 2), confirming the cycloaddition. Significant changes occurred in two regions: 1700–1550 cm⁻¹ and 1500–900 cm⁻¹ (Figure 2). These regions were strongly influenced by the incorporation of the 1,2,3-triazole ring, the benzene ring, and the respective substituents, which altered the peak patterns.

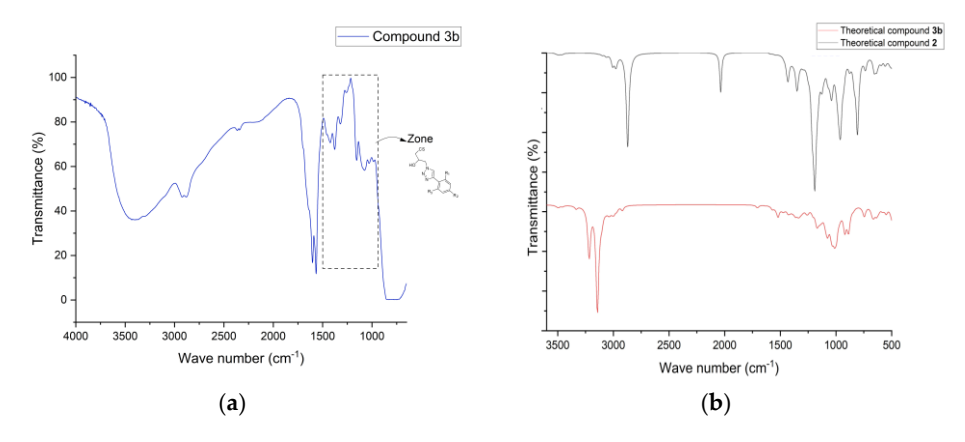


Figure 2. IR spectrum: (a) Experimental spectrum for Compound **3b** (CS-Br); (b) Theoretical spectrum for Compound **3b** (CS-Br) and compound **2** (Azidated chitosan).

Chitosan exhibited an absorption band at 203 nm, located in the UV region, whereas the 1,2,3-triazoles showed absorption in the UV–Vis spectrum, with range into [414.6–457] nm. he cycloaddition introduced triazole rings and alkyne substituents, modifying chromophores and increasing auxochromes, resulting in derivatives (3a–f) with colors from yellow to red.

3.3. Characterization of Films

3.3.1. Mechanical Properties

The chitosan film exhibited lower tensile strength and elongation at break than their derivatives (Figure 3). The incorporation of PVA as a plasticizer reduced intermolecular forces and increased polymer chain mobility, thereby enhancing the flexibility and extensibility of the films [9].

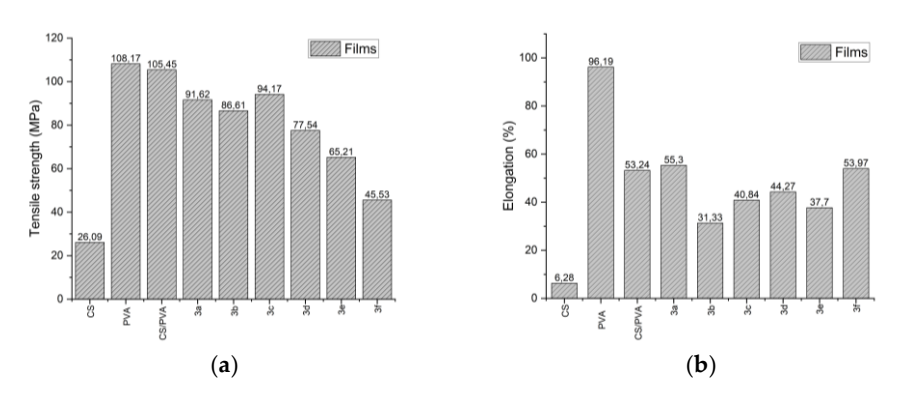


Figure 3. Comparison of mechanical properties of the different films: (a) Tensile strength (b) Elongation.

3.3.2. Thickness

The thicknesses of the films were ranged from 0.0355 to 0.0430 mm. These values indicate that the films can be classified as edible films or coatings. An edible film or coating is defined as any material with a thickness below 0.3 mm, where materials under 0.025 mm are considered coatings, and thicker materials are classified as films [10].

3.3.3. Topographic Analysis

The topographic analysis revealed that films prepared from compounds **3a–f** and PVA exhibited lower surface roughness compared to films of chitosan, PVA, or chitosan blended with PVA (Figure 4). These results are consistent with the surface images obtained by AFM (Figure 4).

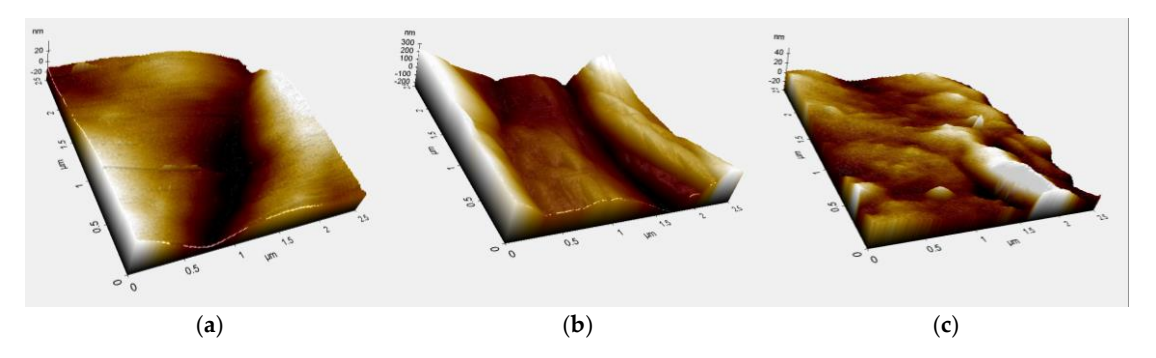


Figure 4. Topographic analysis of the different films by AFM: (a) Chitosan (b) Chitosan/PVA (c) CS-Br.

The mean roughness (Ra) and root mean square roughness (Rq) of compounds **3b**, **3e**, and **3f** were lower than those of unmodified chitosan or PVA (Table 2), indicating smoother surfaces that can minimize gas and moisture permeability. Such smooth surfaces also facilitate the uniform application of coatings, including antimicrobial or biodegradable layers, thereby enhancing the functionality of the films [1].

Compound	Ra (nm)	Rq (nm)
CS	11.29	14.17
PVA	89.57	106.79
CS/PVA	4.90	6.80
CS-TOL (3a)	12.85	15.45
CS-Br (3b)	6.57	9.09
CS-CH ₃ (3c)	13.64	15.67
CS-CHO (3d)	45.63	54.82
CS-CF ₃ (3e)	3.81	4.67
CS-ACN (3f)	5.91	8.12

Table 2. Roughness of different films.

3.3.4. Water Vapor Permeability

Chitosan and PVA films exhibited the highest permeability values, indicating relatively low water barrier properties (Figure 5). This behavior is attributed to the abundance of hydroxyl and amino groups in their molecular structure, which readily interact with water molecules and facilitate their permeation through the films [8].

In contrast, a notable decrease in permeability was observed for the CS-Br and CS-CF3 films (Figure 5). This effect is mainly associated with the presence of bromine and fluorine atoms in their structures. Halogen atoms increase molecular lipophilicity and

hydrophobicity, thereby hindering the diffusion of water molecules through the films and enhancing their barrier properties [11].

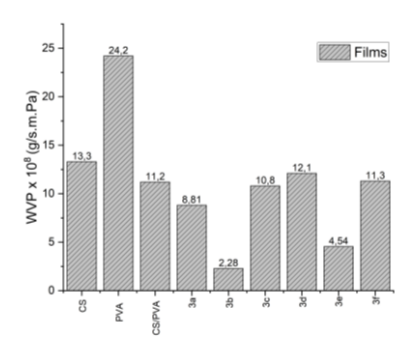


Figure 5. Comparison of the water vapor permeability of different films.

3.3.5. Thermal Stability

Figure 6 shows the thermograms of the films. Chitosan exhibited an endothermic peak at 112 °C (evaporation of water and acetic acid), a Tg at 187.38 °C, and an exothermic peak at 289.16 °C corresponding to thermal decomposition, consistent with previously reported values [12,13]. PVA films presented peaks at 51.29 °C, 81.16 °C, 219.61 °C, and 311.04 °C, associated with Tg, water loss, melting, and decomposition, in agreement with the literature [14]. Chitosan derivatives showed endothermic peaks related to solvent evaporation and decomposition peaks at 326.12 °C (CS-ACN), 303.49 °C (CS-CH₃), 315.13 °C (CS-CF₃), and 322.84 °C (CS-Br), with Tg values between 214–219 °C, indicating higher thermal stability than native chitosan and slightly greater stability than PVA. In contrast, CS-TOL and CS-CHO decomposed at lower temperatures (294.27 °C and 288.74 °C), reflecting reduced stability.

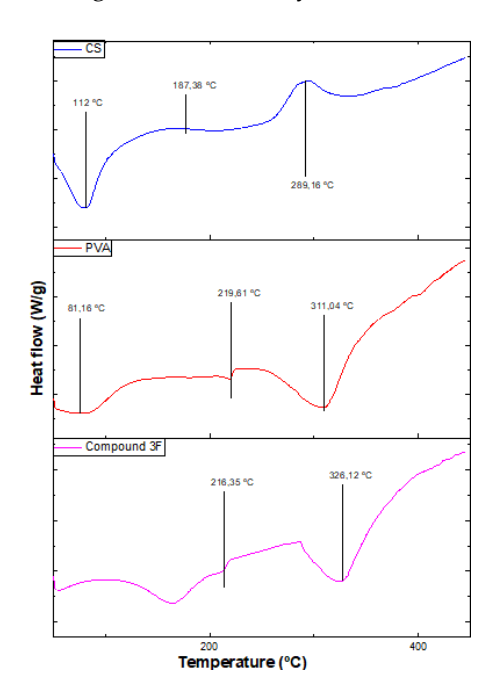


Figure 6. Comparison of thermograms of different films for Chitosan, PVA and compound 3f.

4. Conclusions

In this study, chitosan-triazole derivatives were efficiently synthesized via CuAAC (79.7–88.0% yield) and characterized spectroscopically. Their PVA-based films showed

improved mechanical, structural, and barrier properties, highlighting potential as food coatings.

Author Contributions: Conceptualization, J.G.-G., C.D.A.-L. and P.M.B.-V.; methodology, J.G.-G. and C.D.A.-L.; investigation, J.G.-G.; resources, V.J.T.-T. and R.F.; writing—review and editing, J.G.-G. and C.D.A.-L.; supervision, C.D.A.-L.; project administration, C.D.A.-L. All authors have read and agreed to the published version of the manuscript.

Funding: This research received no external funding

Institutional Review Board Statement: Not applicable.

Informed Consent Statement: Not applicable.

Data Availability Statement: All data generated or analyzed during this study are included in this published article.

Conflicts of Interest: The authors declare no conflicts of interest.

References

- 1. Jasrotia, S.; Gupta, S.; Kudipady, M.L.; Puttaiahgowda, Y.M. Development and Characterization of Chitosan–PVA–Tannic Acid Film for Extended Shelf Life and Safety of Food Products. *ACS Omega* **2025**, *10*, 19361–19378.
- 2. Aguirre-Pranzoni, C.; García, M.G.; Ochoa, N.A. Structural and Conformational Changes on Chitosan after Green Heterogeneous Synthesis of Phenyl Derivatives. *Carbohydr. Polym.* **2023**, *312*, 120843.
- 3. Argüelles-Monal, W.M.; Lizardi-Mendoza, J.; Fernández-Quiroz, D.; Recillas-Mota, M.T.; Montiel-Herrera, M. Chitosan Derivatives: Introducing New Functionalities with a Controlled Molecular Architecture for Innovative Materials. *Polymers* **2018**, *10*, 342.
- 4. Agrahari, A.K.; Bose, P.; Jaiswal, M.K.; Rajkhowa, S.; Singh, A.S.; Hotha, S.; Mishra, N.; Tiwari, V.K. Cu(I)-Catalyzed Click Chemistry in Glycoscience and Their Diverse Applications. *Chem. Rev.* **2021**, *121*, 7638–7956.
- 5. Khan, S.A.; Akhtar, M.J.; Gogoi, U.; Meenakshi, D.U.; Das, A. An Overview of 1,2,3-Triazole-Containing Hybrids and Their Potential Anticholinesterase Activities. *Pharmaceuticals* **2023**, *16*, 179.
- 6. Pozo Llumiquinga, A.Y. Síntesis de derivados de 1, 2, 3 triazol-quitosano a partir de reacciones de clicloadición azida- alquil benceno para aplicaciones en empaques alimenticios. Bachelor Thesis, Universidad Central del Ecuador, Quito, Ecuador, 2022.
- 7. Ullah, A.; Khan, N.R.; Khan, M.H.; Mehmood, S.; Khan, J.; Iftikhar, T.; Gul, I.U.; Basit, H.M.; Qayum, M.; Shah, S.U. Formulation of Microwave-Assisted Natural-Synthetic Polymer Composite Film and Its Physicochemical Characterization. *Int. J. Polym. Sci.* **2021**, 2021, 9961710.
- 8. Cazón, P.; Morales-Sanchez, E.; Velazquez, G.; Vázquez, M. Measurement of the Water Vapor Permeability of Chitosan Films: A Laboratory Experiment on Food Packaging Materials. *J. Chem. Educ.* **2022**, *99*, 2403–2408.
- 9. Sánchez, L.A.P.; Ballén, A.B.; Marchand, L.C.S. Preparación y caracterización de una película de quitosano plastificado: un biomaterial de gran potencial en el campo de la medicina. *Reto* **2019**, *7*, 11–24.
- 10. Priya, K.; Thirunavookarasu, N.; Chidanand, D.V. Recent Advances in Edible Coating of Food Products and Its Legislations: A Review. *J. Agric. Food Res.* **2023**, *12*, 100623.
- 11. Priimagi, A.; Cavallo, G.; Metrangolo, P.; Resnati, G. The Halogen Bond in the Design of Functional Supramolecular Materials: Recent Advances. *Acc. Chem. Res.* **2013**, *46*, 2686–2695.
- 12. Sakurai, K.; Maegawa, T.; Takahashi, T. Glass Transition Temperature of Chitosan and Miscibility of Chitosan/Poly(*N*-Vinyl Pyrrolidone) Blends. *Polymer* **2000**, *41*, 7051–7056.
- 13. Dong, Y.; Ruan, Y.; Wang, H.; Zhao, Y.; Bi, D. Studies on Glass Transition Temperature of Chitosan with Four Techniques. *J. Appl. Polym. Sci.* **2004**, *93*, 1553–1558.
- 14. Remiš, T.; Bělský, P.; Kovářík, T.; Kadlec, J.; Ghafouri Azar, M.; Medlín, R.; Vavruňková, V.; Deshmukh, K.; Sadasivuni, K.K. Study on Structure, Thermal Behavior, and Viscoelastic Properties of Nanodiamond-Reinforced Poly (Vinyl Alcohol) Nanocomposites. *Polymers* **2021**, *13*, 1426.

Disclaimer/Publisher's Note: The statements, opinions and data contained in all publications are solely those of the individual author(s) and contributor(s) and not of MDPI and/or the editor(s). MDPI and/or the editor(s) disclaim responsibility for any injury to people or property resulting from any ideas, methods, instructions or products referred to in the content.